# What a Single Electroencephalographic (EEG) Channel Can Tell us About Alzheimer's Disease Patients With Mild Cognitive Impairment

**Claudio Del Percio**[1,†] (iD), **Susanna Lopez**[1,†] (iD), **Giuseppe Noce**[2],
**Roberta Lizio**[2], **Federico Tucci**[1], **Andrea Soricelli**[2,3], **Raffaele Ferri**[4],
**Flavio Nobili**[5,6], **Dario Arnaldi**[5,6], **Francesco Famà**[5], **Carla Buttinelli**[7],
**Franco Giubilei**[7], **Moira Marizzoni**[8], **Bahar Güntekin**[9,10] (iD),
**Görsev Yener**[11] (iD), **Fabrizio Stocchi**[12], **Laura Vacca**[12],
**Giovanni B. Frisoni**[8,13], and **Claudio Babiloni**[1,14]

## Abstract

Abnormalities in cortical sources of resting-state eyes closed electroencephalographic (rsEEG) rhythms recorded by hospital settings (10-20 montage) with 19 scalp electrodes characterized Alzheimer's disease (AD) from preclinical to dementia stages. An intriguing rsEEG application is the monitoring and evaluation of AD progression in large populations with few electrodes in low-cost devices. Here we evaluated whether the above-mentioned abnormalities can be observed from fewer scalp electrodes in patients with mild cognitive impairment due to AD (ADMCI). Clinical and rsEEG data acquired in hospital settings (10-20 montage) from 75 ADMCI participants and 70 age-, education-, and sex-matched normal elderly controls (Nold) were available in an Italian-Turkish archive (PDWAVES Consortium; www.pdwaves.eu). Standard spectral fast fourier transform (FFT) analysis of rsEEG data for individual delta, theta, and alpha frequency bands was computed from 6 monopolar scalp electrodes to derive bipolar C3-P3, C4-P4, P3-O1, and P4-O2 markers. The ADMCI group showed increased delta and decreased alpha power density at the C3-P3, C4-P4, P3-O1, and P4-O2 bipolar channels compared to the Nold group. Increased theta power density for ADMCI patients was observed only at the C3-P3 bipolar channel. Best classification accuracy between the ADMCI and Nold individuals reached 81% (area under the receiver operating characteristic curve) using Alpha2/Theta power density computed at the C3-P3 bipolar channel. Standard rsEEG power density computed from six posterior bipolar channels characterized ADMCI status. These results may pave the way toward diffuse clinical applications in health monitoring of dementia using low-cost EEG systems with a strict number of electrodes in lower- and middle-income countries.

[1]Department of Physiology and Pharmacology "Vittorio Erspamer", Sapienza University of Rome, Rome, Italy
[2]IRCCS Synlab SDN, Naples, Italy
[3]Department of Motor Sciences and Healthiness, University of Naples Parthenope, Naples, Italy
[4]Oasi Research Institute - IRCCS, Troina, Italy
[5]Clinica neurologica, IRCCS Ospedale Policlinico San Martino, Genova, Italy
[6]Dipartimento di Neuroscienze, Oftalmologia, Genetica, Riabilitazione e Scienze Materno-infantili (DiNOGMI), Università di Genova, Italy
[7]Department of Neuroscience, Mental Health and Sensory Organs, Sapienza University of Rome, Rome, Italy
[8]Laboratory of Alzheimer's Neuroimaging and Epidemiology, IRCCS Istituto Centro San Giovanni di Dio Fatebenefratelli, Brescia, Italy
[9]Department of Biophysics, School of Medicine, Istanbul Medipol University, Istanbul, Turkey
[10]REMER, Clinical Electrophysiology, Neuroimaging and Neuromodulation Lab., Istanbul Medipol University, Istanbul, Turkey
[11]Izmir University of Economics, Faculty of Medicine, Izmir, Turkey
[12]IRCCS San Raffaele, Rome, Italy
[13]Memory Clinic and LANVIE - Laboratory of Neuroimaging of Aging, University Hospitals and University of Geneva, Geneva, Switzerland
[14]Hospital San Raffaele Cassino, Cassino (FR), Italy

[†]Equally contributing first author.

**Corresponding Author:**
Claudio Del Percio, Department of Physiology and Pharmacology "V. Erspamer", Sapienza University of Rome, P. le A. Moro 5, 00185, Rome, Italy.
Email: claudio.delpercio@uniroma1.it
Full-color figures are available online at journals.sagepub.com/home/eeg

## Introduction

According to the Alzheimer's Association International (https://www.alzint.org) annual reports, dementia causes severe cognitive deficits, disability, and dependency in daily living in about 55 million older adults, with no effective disease-modifying drug available and annual costs of > > $1 trillion worldwide. Neurodegenerative Alzheimer's disease (AD) is the most prevalent cause of dementia. It is characterized by the abnormal progressive (neurotoxic) accumulation of amyloid and tau proteins in the brain over about ten years. An anti-amyloid vaccination trial named "Aducanumab" may be able to treat AD and is under clinical verification (https://www.alzforum.org/therapeutics/aduhelm). Hence, the early identification and monitoring of AD patients are increasingly important.

US National Institute of Aging and Alzheimer's Association recently proposed a new diagnostic gold standard for AD research.[1] Experts of those institutions distinguished two different levels of the diagnosis: the determination of the clinical syndrome and the in-vivo identification of the neuropathological disease-inducing that syndrome.[1] The following stages of disease severity characterized the clinical syndrome based on standard neuropsychological tests and clinical scales: an absence of cognitive deficits (preclinical stage), mild cognitive deficits (MCI, prodromal stage of dementia), and dementia. From a neuropathological point of view, AD was in-vivo diagnosed by abnormal accumulation of amyloid and tau proteins in the brain, as revealed by cerebrospinal fluid (CSF) measures or positron emission tomography (PET) imaging.[1] This theoretical framework predicts that this AD-related abnormal accumulation induces progressive neurodegenerative processes in the brain, as revealed by structural magnetic resonance imaging (sMRI) or Fluorodeoxyglucose-PET and the clinical syndrome.[1] According to this theoretical framework, AD can be diagnosed by the above in-vivo methodologies even when the clinical syndrome shows the MCI condition. For this reason, a new term was introduced referring to both the neuropathological diagnosis of "AD" and the clinical syndrome of "MCI," namely ADMCI.[2]

Notably, CSF, sMRI, and PET imaging are too expensive and invasive for large pre-screening and monitoring of AD over the years in older adults at risk, especially in lower- and middle-income countries and underserved European populations.

To tackle this issue, recording of eyes-closed resting-state electroencephalographic (rsEEG) rhythms in quiet and relaxed wakefulness may represent a promising tool to monitor brain functions over time in serial recordings conducted in AD patients from MCI to dementia.[2] Previous studies using a clinical electrode montage with 19 scalp leads and topographical and frequency analysis of rsEEG activity have shown typical abnormalities in rsEEG rhythms during the AD progression,[2, 3, 4, 5] especially at delta, theta, and alpha bands. As compared to cognitively unimpaired old (Nold) seniors, patients with AD dementia (ADD) showed the following abnormalities: (1) widespread decrease in the magnitude of alpha rhythms; (2) decreased dominant alpha frequency to 8–7 Hz[6]; (3) widespread increase in the magnitude of theta and delta rhythms; and 4) more negligible magnitude reactivity of alpha rhythms during the eye-opening.[6] Those abnormalities were also reported in ADMCI patients[7, 8,9] about the so-called "cognitive reserve" related to years of education,[10] aging,[11] and sex.[12]

Low-cost, portable EEG systems with a small number of scalp electrodes open a new avenue for rsEEG markers. These systems may be readily available in all centers for the evaluation and disease progression monitoring of older adults at risk of dementing disorders in low- and middle-income countries. Previous studies showed that those systems could record rsEEG activity with a good signal-to-noise ratio and reliability in young and old adults.[13–16] However, it is unclear if these differences between Nold seniors and ADMCI patients may be replicated at the group and individual levels when including only a few scalp electrodes to extract rsEEG biomarkers to be used as inputs for statistical models.

In this study, we evaluated the hypothesis that significant abnormalities of rsEEG spectral biomarkers may be found in ADMCI patients over Nold seniors using only 6 monopolar scalp electrodes of 10–20 electrode montage to derive bipolar C3-P3, C4-P4, P3-O1, and P4-O2 leads. We used rsEEG data in Nold and ADMCI patients from an international database (www.pdwaves.eu) and performed a standard spectral FFT analysis of rsEEG activity at individual delta, theta, and alpha frequency bands. Statistical models assessed differences between the Nold and ADMCI persons at both group and individual levels.

Notably, the clinical significance of the present study was to verify whether rsEEG biomarkers acquired from a few scalp electrodes in a standard hospital setting may discriminate between Nold and ADMCI seniors. If confirmed, these results will justify their potential candidature as a "gold standard" for a new generation of rsEEG biomarkers derived from low-cost portable EEG systems characterized by few channels and low energy consumption. This "gold standard" may be a

reference to approximate the performance of those mobile systems to that standard for future applications in extensive elderly population health screening and monitoring of AD and other neurodegenerative disease progressions to timely prevent or at least delay the appearance of clinical symptoms.

## Materials and Methods

### Participants

To evaluate the study hypotheses, clinical, neuropsychological, anthropometric, genetic, cerebrospinal fluid (CSF), MRI, and rsEEG data in 70 Nold and 75 ADMCI subjects from an international archive were used in the present study. The following Italian and Turkish clinical units enrolled the participants: the Sapienza University of Rome (Italy), Institute for Research and Evidence-based Care (IRCCS) "Fatebenefratelli" of Brescia (Italy), IRCCS SDN of Naples (Italy), IRCCS Oasi Maria SS of Troina (Italy), IRCCS Ospedale Policlinico San Martino and DINOGMI (University of Genova, Italy), Hospital San Raffaele of Cassino (Italy), IRCCS San Raffaele Pisana of Rome (Italy) and Medipol University of Istanbul (Turkey).

The two groups (ie, Nold and ADMCI) were carefully matched for age, gender, and education (ie, the mean values of age, gender, and education were not different between these groups). Table 1 summarizes the most relevant demographic (ie, age, gender, and educational attainment) and clinical (ie, mini-mental state evaluation, MMSE, score) features of the Nold and ADMCI groups. Furthermore, Table 1 reports the results of the presence or absence of statistically significant differences ($p < 0.05$) between the two groups for age (T-test), gender (Fisher test), educational attainment (T-test), and MMSE score (Mann Whitney U test). As expected, a statistically significant difference was found for the MMSE score ($p < 0.00001$), showing a higher score in the Nold than the ADMCI group. On the contrary, no statistically significant differences were found for the age, gender, and education attainment between the groups ($p > 0.05$).

Local institutional Ethics Committee approved the present observational study. All experiments were performed with the informed and overt consent of each participant or caregiver, in line with the Code of Ethics of the World Medical Association (Declaration of Helsinki) and the standards established by the local Institutional Review Board.

### Diagnostic Criteria

The status of the ADMCI was based on the "positivity" to Aβ1-42/phospho-tau ratio in the cerebrospinal fluid (CSF). The diagnosis was also supported by one or both biomarkers as revealed by FDG-PET and structural MRI of the hippocampus, parietal, temporal, and posterior cingulate regions.[17] The "positivity" was judged by the physicians in charge of releasing the clinical diagnosis to the patients, according to the local diagnostic routine of the participating clinical Units.

The clinical inclusion criteria of the ADMCI patients were as follows: (1) age of 55–90 years; (2) reported memory complaints by the patient and/or a relative; (3) MMSE score of 24 or higher; (4) Clinical Dementia Rating score of 0.5 (CDR [18]); (5) logical memory test[19] score of 1.5 standard deviations (SD) below the mean adjusted for age; the cognitive deficits did not significantly interfere with the functional independence in the activities of the daily living; (6) Geriatric Depression Scale (15-item GDS [20]) score of 5 or lower; (7) modified Hachinski ischemia[21] score of 4 or lower and education of 5 years or higher; (8) single or multi-domain MCI status, and (9), an objective deficit in episodic memory domain as revealed by immediate and delayed recall of Rey Auditory Verbal Learning Test (AVLT 2;2).

The clinical exclusion criteria of the ADMCI patients were as follows: (1) other significant systemic, psychiatric, neurological illness; (2) mixed dementia; (3) actual participation in a clinical trial using disease-modifying drugs; (4) systematic use of antidepressant drugs with anticholinergic side effects; (5) chronic use of neuroleptics, narcotics, analgesics, sedatives or hypnotics; (6) and anti-parkinsonian medications (cholinesterase inhibitors and Memantine allowed); (7) diagnosis of epilepsy or report of seizures or epileptiform EEG signatures in the past, and (8) major depression disorders described in the Diagnostic and Statistical Manual of Mental Disorders (DSM-5).

**Table 1.** Mean Values (± Standard Error of the Mean, SE) of the Demographic and Clinical Data as Well as the Results of their Statistical Comparisons ($p < 0.05$) in the Groups of Normal old (Nold) Seniors (N = 70) and Patients with Alzheimer's Disease and Mild Cognitive Impairment (ADMCI, N = 75). Legend: MMSE = Mini Mental State Evaluation; M/F = Males/Females.

| Demographic and clinical data in Nold and ADMCI | | | |
|---|---|---|---|
| | Nold | ADMCI | Statistical analysis |
| **N** | 70 | 75 | |
| **Age** | 69.5 ± 0.9 | 69.7 ± 0.7 | T test: n.s. |
| **Gender (M/F)** | 28/42 (40% male) | 32/43 (43% male) | Fisher test: n.s. |
| **Education** | 11.0 ± 0.5 | 11.1 ± 0.5 | T test: n.s. |
| **MMSE** | 28.7 ± 0.1 | 25.1 ± 0.2 | Mann Whitney U test: p < 0.0001 |

In all ADMCI patients, Apolipoprotein E (ie, APOE) genotyping and CSF biomarkers were assessed. CSF was preprocessed, frozen, and stored in line with the Alzheimer's Association Quality Control Programme for CSF biomarkers.[23] Levels of amyloid beta 1–42 (ie, Aβ42), protein tau (ie, total tau, t-tau), and phosphorylated form of tau (ie, p-tau) were also measured. Moreover, anthropometric features (ie, weight, height, and body mass index) and cardiocirculatory markers (ie, systolic pressure, diastolic pressure, pulse pressure, mean arterial pressure, and heart frequency) were also taken into consideration in the analysis.

Furthermore, in all ADMCI patients, the performance in various cognitive domains, including global cognitive status, memory, language, executive function, planning, visuospatial function, and attention was assessed by the following materials: (1) the global cognitive status was tested by the mini mental state evaluation exam (MMSE) and the Alzheimer's Disease Assessment Scale–Cognitive Subscale (ADAS-Cog[24,25]); (2) the episodic memory was assessed by the immediate and delayed recall of Rey Auditory Verbal Learning Test[26]; (3) the executive functions and attention were evaluated by the Trail making test (TMT) part A and B[27]; (4) the language was tested by 1-min Verbal fluency test for letters[28] and 1-min Verbal fluency test for category (fruits, animals or car trades 2;8); and (5) planning abilities and visuospatial functions were assessed by Clock drawing and copy test.[29]

In the present ADMCI cohort, the mean score for the baseline episodic memory deficit, as revealed by the immediate and delayed recall of the Rey Auditory Verbal Learning Test, was $28.9 \pm 1.1$ and $4.2 \pm 0.7$, respectively, both under the cut-off scores in relation to 60–69 years of age.[30] Furthermore, after 12 months, the decline in MMSE score was $-1.2 \pm 0.3$, the decline in the immediate recall of AVLT score was $-0.37 \pm 0.83$ and the decline in the delayed recall of AVLT score was $-1.28 \pm 0.68$. A statistically significant difference was observed between the baseline and the 12-month follow-up delayed recall of AVLT score (Wilcoxon Matched Pairs Test; $p < 0.01$; $Z = 2.60$).

Moreover, in all ADMCI patients, drugs were withdrawn for about 24 h before rsEEG recordings. This act did not ensure a complete drug washout for obvious ethical reasons. This procedure enabled the comparison of rsEEG data while maintaining treatment in the ADMCI patients. We checked the administration of psychoactive drugs for mental disorders (ie, sedatives, anxiolytics, antidepressants, antipsychotics) and medications for AD treatment (eg, acetylcholinesterase inhibitors) in all ADMCI patients. The following ADMCI patients assumed psychoactive medications for mental disorders before the EEG recordings: drugs for anxiety and depression (Sertraline, Escitalopram, Citalopram, Paroxetine, Venflaxine, Duloxetine) = 26, antipsychotic drugs (Bromazepam, Alprazolam) = 2, dementia drugs (Donepezil, Rivastigmine, Memantine, Galantamine) = 16.

All Nold subjects underwent cognitive screening (including MMSE and GDS) as well as physical and neurological examinations to exclude subjective memory complaint, cognitive deficits, and mood disorders. All Nold subjects had a GDS score lower than the threshold of 6 (no depression) or no depression after an interview with a physician or clinical psychologist at the time of the enrolment. The Nold subjects with a history of previous or present neurological or psychiatric disease were also excluded. Furthermore, the Nold subjects affected by any chronic systemic illnesses (eg, diabetes mellitus) were excluded, as were the Nold subjects taking chronically psychoactive drugs.

## The Resting State Electroencephalographic (rsEEG) Recordings

The rsEEG activity was recorded while the subjects were relaxed with eyes closed on a comfortable reclined chair. Instructions for rsEEG recordings encouraged the subjects to experience quiet wakefulness with muscle relaxation, no voluntary movements, no talking, and no development of systematic goal-oriented mentalization. Rather, a quiet wandering mode of mentalization was kindly required.

In all subjects, rsEEG recordings lasted about 3–5 min. The rsEEG data were recorded with a sampling frequency of 128–512 Hz and related antialiasing bandpass between 0.01 Hz and 60–100 Hz. Electrode montage included 19 scalp monopolar sensors placed following 10–20 System (ie, O1, O2, P3, Pz, P4, T3, T5, T4, T6, C3, Cz, C4, F7, F3, Fz, F4, F8, Fp1, and Fp2). A frontal ground electrode was used, while cephalic or linked earlobe electrodes were used as electric references according to local methodological facilities and standards. Electrodes impedances were kept below 5 kΩ. Vertical and horizontal electro-oculographic (EOG) potentials (0.3-70 Hz bandpass) were recorded to control eye movements and to blink.

## The rsEEG Preliminary Data Analysis

The preliminary analysis of the recorded rsEEG activity followed the same procedures of previous rsEEG investigations in MCI patients of our Workgroup[31–33] to make comparable the results.

For this analysis, the rsEEG data were divided into epochs of 2 s and analyzed offline as follows. The rsEEG epochs affected by any physiological (ocular/ blinking, muscular, and head movements) or non-physiological (sweat, bad contact between electrodes and scalp, etc) artefacts were identified and discarded by the visual analysis of two experts of EEG signals (C.D.P., S.L., G.N., or R.L.). In this visual analysis, the contamination of rsEEG rhythms with the ocular activity (ie, blinking) was evaluated in frontal electrodes (ie, F7, F3, Fz, F4, F8, Fp1, and Fp2), comparing EOG and EEG traces. Head movement artefacts were detected by a sudden and great increase in amplitude of slow EEG waves in all scalp electrodes. Muscle tension artefacts were recognized by observing the effects of frequency bandpass filters in different ranges and by the inspection of rsEEG power density spectra. These

artefacts were reflected by unusually high and stable values of rsEEG power density from 30 to 100 Hz, which contrast with the typical declining trend of rsEEG power density from 25 Hz onward. The experimenters also detected rsEEG epochs with signs of sleep such as K complexes, sleep spindles, vertex shape waves, and slow waves. Furthermore, the two experimenters carefully rejected rsEEG epochs associated with behavioral annotations taken during the experiments (eg, drowsiness, verbal warnings, opened eyes, arm/hand movements, etc).

After the above procedures, the artefact-free epochs showed the same proportion of the total amount of rsEEG activity recorded in both ADMCI and Nold groups (> 85%). A statistical procedure (T-tests) showed no statistically significant difference ($p > 0.05$) for artefact-free epochs between the two groups (Nold vs ADMCI: $p = 0.4$).

To test the main hypothesis of the present study, we extracted the following centro-parietal and parieto-occipital bipolar rsEEG signals by re-referencing the first to the second channel:

- Bipolar C3-P3,
- Bipolar C4-P4,
- Bipolar P3-O1, and
- Bipolar P4-O2.

## The Spectral Analysis of rsEEG Epochs

A standard digital FFT-based analysis (Welch technique, Hanning windowing function, no phase shift) used the rsEEG epochs free from artefacts to compute the power density of scalp rsEEG rhythms (0.5 Hz of frequency resolution) of the above-mentioned bipolar channels. We used the official freeware tool called exact low-resolution brain electromagnetic tomography (eLORETA) for the bipolar rsEEG spectral power density estimation.[34]

The EEG frequency bands of interest were individually identified based on the following frequency landmarks, namely the transition frequency (TF) and IAFp.[35, 36] In the EEG power density spectrum, the TF marks the transition frequency between the theta and alpha bands, defined as the minimum of the rsEEG power density between 3 and 8 Hz (between the delta and the alpha power peak). The IAF is defined as the maximum power density peak between 6 and 14 Hz. These frequency landmarks were previously well described by Dr Wolfgang Klimesch.[36–38]

The TF and IAF were computed for each subject involved in the study. Based on the TF and IAF, we estimated the individual delta, theta, and alpha bands as follows: delta from TF $-4$ Hz to TF $-2$ Hz, theta from TF $-2$ Hz to TF, low-frequency alpha (alpha 1 and alpha 2) from TF to IAF, and high-frequency alpha (or alpha 3) from IAF to IAF $+ 2$ Hz. Specifically, the individual alpha 1 and alpha 2 bands were computed as follows: alpha 1 from TF to the frequency midpoint of the TF-IAF range and alpha 2 from that midpoint to IAF. The other bands were defined based on the standard fixed frequency ranges used in the reference study[11]: beta 1 from 14 to 20 Hz, beta 2 from 20 to 30 Hz, and gamma from 30 to 40 Hz.

Of note, important aspects of the procedure were the following: (1) we divided the alpha band into sub-bands because, in the eyes-closed rsEEG condition, dominant low-frequency alpha rhythms (alpha 1 and alpha 2) may denote the synchronization of diffuse neural networks regulating the fluctuation of the subject's global awake and conscious states, while high-frequency alpha rhythms (alpha 3) may denote the synchronization of more selective neural networks specialized in the processing of modal specific or semantic information.[35, 39] When the subject is engaged in sensorimotor or cognitive tasks, alpha and low-frequency beta (beta 1) rhythms reduce in power (ie, desynchronization or blocking) and are replaced by fast EEG oscillations at high-frequency beta (beta 2) and gamma rhythms[39]; (2) we considered individual delta, theta, and alpha frequency bands because of a clinical group may be characterized by a mean slowing in the peak frequency of the alpha power density without any substantial change in the magnitude of the power density. In that specific case, the use of fixed frequency bands would result in a statistical effect erroneously showing alpha power density values lower in the clinical than the control group; (3) we used fixed frequency ranges for the beta and gamma bands because of the individual beta and gamma frequency peaks were evident only in a few subjects (< 10%); (4) we selected the beginning of the beta frequency range at 14 Hz to avoid the overlapping between individual alpha and fixed beta frequency ranges (ie, individual alpha frequency band ranged from TF to 14 Hz with an IAF $= 12$ Hz).

## Statistical Analysis of the Bipolar rsEEG Spectral Power Density

Two statistical sessions were performed by the commercial tool STATISTICA 10 (StatSoft Inc., www.statsoft.com) to evaluate the study hypotheses. In all statistical sessions, an ANOVA was computed using the bipolar rsEEG spectral power density as dependent variable (one ANOVA for each bipolar rsEEG signal; $p < 0.05$). It is well-known that the use of ANOVA models implies that dependent variables approximate Gaussian distributions, so we tested this feature in the bipolar rsEEG spectral power density by Kolmogorov-Smirnov test (null hypothesis of non-Gaussian distributions tested at $p > 0.05$). As the distributions of the bipolar rsEEG spectral power density were not Gaussian in all cases, those values underwent the log-10 transformation and were re-tested. Such a transformation is a popular method to transform skewed data distribution with all positive values (as bipolar rsEEG spectral power density values are) to Gaussian distributions, thus augmenting the reliability of the ANOVA results. Indeed, the procedure approximated the distributions of all eLORETA solutions to Gaussian distributions ($p > 0.05$), allowing the use of the ANOVA model.

Mauchly's test evaluated the sphericity assumption, and degrees of freedom were corrected by the Greenhouse-Geisser procedure when appropriate ($p < 0.05$). Duncan test was used for post-hoc comparisons ($p < 0.05$, corrected for multiple comparisons).

The results of the following statistical analyses were controlled by the iterative (leave-one-out) Grubbs' test detecting the presence of one or more outliers in the distribution of the bipolar rsEEG spectral power density values. We tested the null hypothesis of the non-outlier status at the arbitrary threshold of $p > 0.001$ to remove only individual values with a high probability of being outliers.

The first four ANOVAs tested the hypothesis that the bipolar rsEEG spectral power density at delta and alpha frequencies were abnormal in the ADMCI patients as compared to the Nold seniors (one ANOVA for each bipolar rsEEG spectral power density). The ANOVA factors were Group (Nold and ADMCI) and Band (delta, theta, alpha 1, alpha 2, alpha 3, beta 1, beta 2, and gamma). The confirmation of the hypothesis would require: (1) a statistically significant ANOVA interaction including the factors Group and Band ($p < 0.05$) and (2) a post-hoc Duncan test indicating statistically significant ($p < 0.05$ Bonferroni corrected) differences in the rsEEG source activities at delta, theta, and alpha frequencies between the Nold and ADMCI groups (ie, Nold $\neq$ ADMCI, $p < 0.05$ Bonferroni corrected).

The second four ANOVAs tested the hypothesis that composite ratio biomarkers of bipolar rsEEG spectral power density were abnormal in the ADMCI patients as compared to the Nold seniors (one ANOVA for each bipolar rsEEG spectral power density). The composite biomarkers were calculated as follows: ratio between alpha 2 and delta (A2/De), ratio between alpha 3 and delta (A3/De), ratio between alpha 2 and theta (A2/Th), and ratio between alpha 3 and theta (A3/Th) bipolar rsEEG spectral power density. The ANOVA factors were Group (Nold and ADMCI) and Biomarkers (A2/De, A3/De, A2/Th, and A3/Th). The confirmation of the hypothesis would require: (1) a statistically significant ANOVA interaction including the factors Group and Biomarkers ($p < 0.05$) and (2) a post-hoc Duncan test indicating statistically significant ($p < 0.05$ Bonferroni corrected) differences in the composite ratio biomarkers of bipolar rsEEG spectral power density between the Nold and ADMCI groups (ie, Nold $\neq$ ADMCI, $p < 0.05$ Bonferroni corrected).

### Classification at the Individual Level with ROC Curve

The delta, theta, alpha and composite ratio biomarkers of bipolar rsEEG spectral power density were used as discriminant ($\neq$ "diagnostic") variables to classify between the ADMCI and Nold individuals. We computed the receiver-operating characteristic (ROC [40]) curves by GraphPad Prism software (GraphPad Software, Inc., California, USA). The sensitivity (ie, true positive rate), specificity (ie, true negative rate), accuracy (ie, the weighted average of the sensitivity and specificity

values), and area under the ROC (AUROC) curve provided the measure of the classification performance. We used the AUROC curve to assess the excellence of classification. AUROC values higher than 0.7 correspond to a moderate to a good performance of the classification.

As a methodological remark, the general use of a liberal statistical threshold ($p < 0.05$) reflects the preliminary and exploratory nature of the present study from a forward-looking perspective of future longitudinal rsEEG studies in ADMCI patients.

## Results

### Bipolar rsEEG Spectral Power Density in in the Patients with Alzheimer's Disease Mild Cognitive Impairment (ADMCI) and Normal Elderly Subjects (Nold)

Table 2 reports the mean values of TF and IAF for the Nold and ADMCI groups of the bipolar rsEEG spectral power density evaluated for the selected centro-parietal and parieto-occipital channels, together with the results of the statistical comparisons between them (T-test). The statistical threshold was set at $p < 0.025$ (ie, 2 markers, $p < 0.05/2 = 0.025$) to obtain the Bonferroni correction at $p < 0.05$. The T-tests showed that only the mean IAF ($p < 0.001$) values were statistically lower in the ADMCI than the Nold group. These findings emphasized the importance of the use of the TF and IAF in the determination of the delta to alpha frequency bands in the studies involving ADMCI patients.

Figure 1 shows the mean values ($\pm$ SE, log-10 transformed) of the bipolar rsEEG spectral power density evaluated for the selected centro-parietal and parieto-occipital channels. The four sub-figures illustrate statistically significant ANOVA interaction effects ($p < 0.0001$; Fisher test values reported in each sub-figure) among the factors Group (Nold and ADMCI) and

**Table 2.** Mean Values ($\pm$ SE) of Transition Frequency (TF) and Individual Alpha Frequency Peak (IAF) Computed from Bipolar rsEEG Power Density Spectra Estimated at the Four Centro-Parietal and Parieto-Occipital Bipolar Channels (C3-P3, C4-P4, P3-O1, and P4-O2) in the ADMCI (N = 75) and Nold (N = 70) Groups. The Results of the Presence or Absence of Statistically Significant Differences (T test, $p < 0.05$ Corrected) Between the Two Groups are Also Reported.

| | | Nold | ADMCI | T test |
|---|---|---|---|---|
| **Bipolar** | **TF** | $5.3 \pm 0.1$ | $5.1 \pm 0.1$ | n.s. |
| **C3-P3** | **IAF** | $9.4 \pm 0.1$ | $8.6 \pm 0.2$ | $p < 0.001$ |
| **Bipolar** | **TF** | $5.5 \pm 0.1$ | $5.1 \pm 0.1$ | n.s. |
| **C4-P4** | **IAF** | $9.5 \pm 0.1$ | $8.7 \pm 0.2$ | $p < 0.001$ |
| **Bipolar** | **TF** | $5.3 \pm 0.1$ | $5.1 \pm 0.1$ | n.s. |
| **P3-O1** | **IAF** | $9.4 \pm 0.1$ | $8.9 \pm 0.2$ | $p < 0.02$ |
| **Bipolar** | **TF** | $5.4 \pm 0.1$ | $5.1 \pm 0.1$ | n.s. |
| **P4-O2** | **IAF** | $9.3 \pm 0.1$ | $8.8 \pm 0.2$ | $p < 0.02$ |
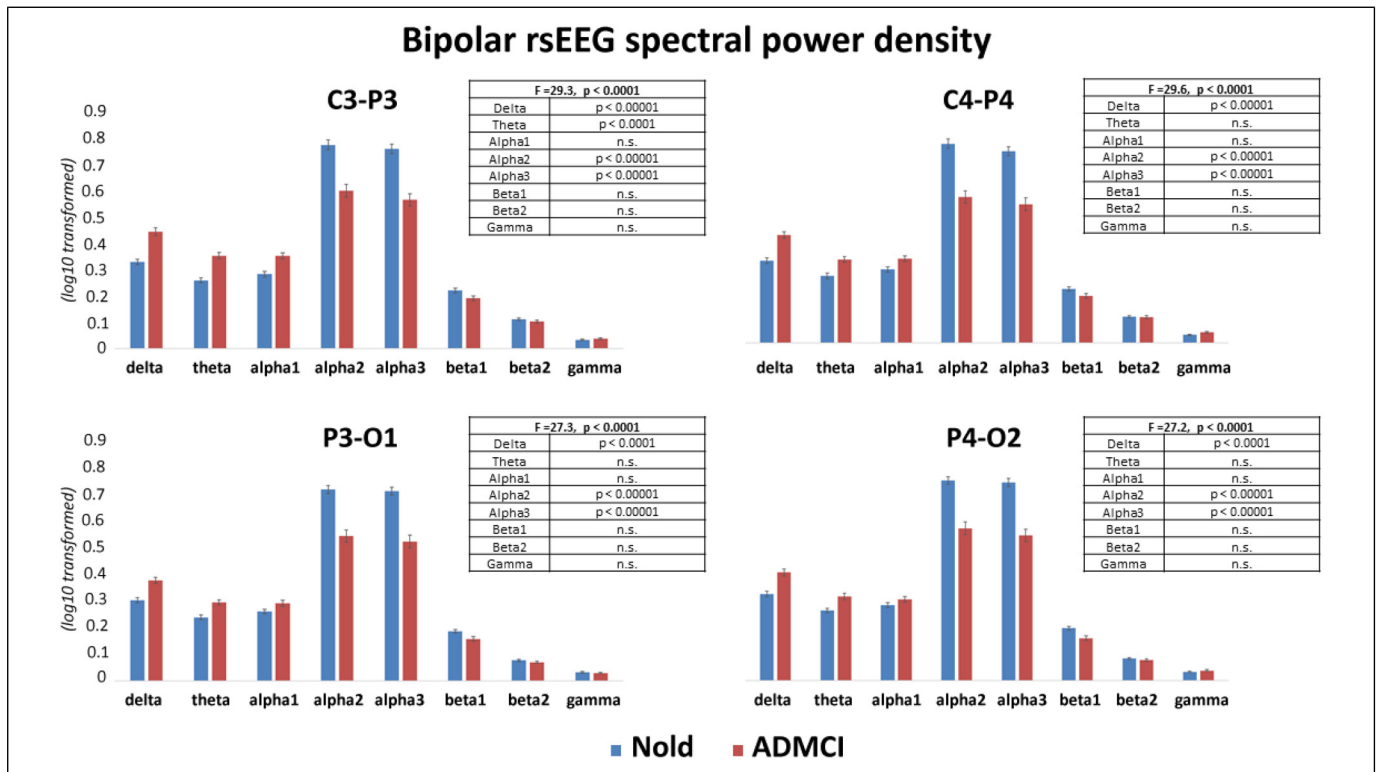
**Figure 1.** Bipolar rsEEG spectral power density estimated at the four centro-parietal and parieto-occipital bipolar channels (C3-P3, C4-P4, P3-O1, and P4-O2; mean across subjects, log-10 transformed) relative to statistically significant ANOVA interactions (p < 0.0001; Fisher test values reported in each sub-figure) among the factors Group (Nold and ADMCI) and Band (delta, theta, alpha 1, alpha 2, alpha 3, beta 1, beta 2, and gamma). Legend: the tables in each sub-figure indicate the frequency bands in which the Bipolar rsEEG spectral power density differed between Nold and ADMCI groups (p < 0.05 corrected = p < 0.00625).

Band (delta, theta, alpha 1, alpha 2, alpha 3, beta 1, beta 2, and gamma). In the Nold group, the bipolar rsEEG spectral power density showed maximum values for the alpha 2 and alpha 3 frequencies. Compared to Nold, the ADMCI group showed a substantial decrease of these values and a substantial increase in the bipolar rsEEG spectral power density in delta and theta frequencies. These results were observable for all the selected centro-parietal and parieto-occipital channels (Duncan planned post-hoc, p < 0.05 Bonferroni correction for 8 frequency bands, p < 0.00625). Of note, these findings were not due to outliers from those individual bipolar rsEEG spectral power density (log-10 transformed), as shown by Grubbs' test with an arbitrary threshold of p > 0.001 (see Figure 2).

## Composite Ratio Biomarkers of Bipolar rsEEG Spectral Power Density in ADMCI and Nold Groups

Figure 3 shows the mean values (± SE, log-10 transformed) of the composite ratio biomarkers of the bipolar rsEEG spectral power density (ie, A2/De, A3/De, A2/Th, and A3/Th) evaluated for the selected centro-parietal and parieto-occipital channels. The four sub-figures illustrate statistically significant ANOVA interaction effects (p < 0.0001 to p < 0.05; Fisher

test values reported in each sub-figure) among the factors Group (Nold and ADMCI) and Biomarkers (A2/De, A3/De, A2/Th, and A3/Th). Compared to Nold, the ADMCI group showed a substantial decrease of all these composite ratio biomarkers of the bipolar rsEEG spectral power density. These results were observable for all the selected centro-parietal and parieto-occipital channels (Duncan planned post-hoc, p < 0.05 Bonferroni correction for 4 biomarkers, p < 0.0125). Of note, these findings were not due to outliers from those individual composite ratio biomarkers of the bipolar rsEEG spectral power density (log-10 transformed), as shown by Grubbs' test with an arbitrary threshold of p > 0.001 (see Figure 4).

## Analyses at the Individual Level

As planned, the delta, theta, alpha and composite ratio biomarkers of bipolar rsEEG spectral power density (log-10 transformed) were used as discriminant input variables for the computation of the AUROC curves. Core results showed that the best discriminant accuracy (AUROC curve) was reached in the discrimination between the ADMCI and Nold individuals at by the composite ratio biomarkers including theta, alpha 2,
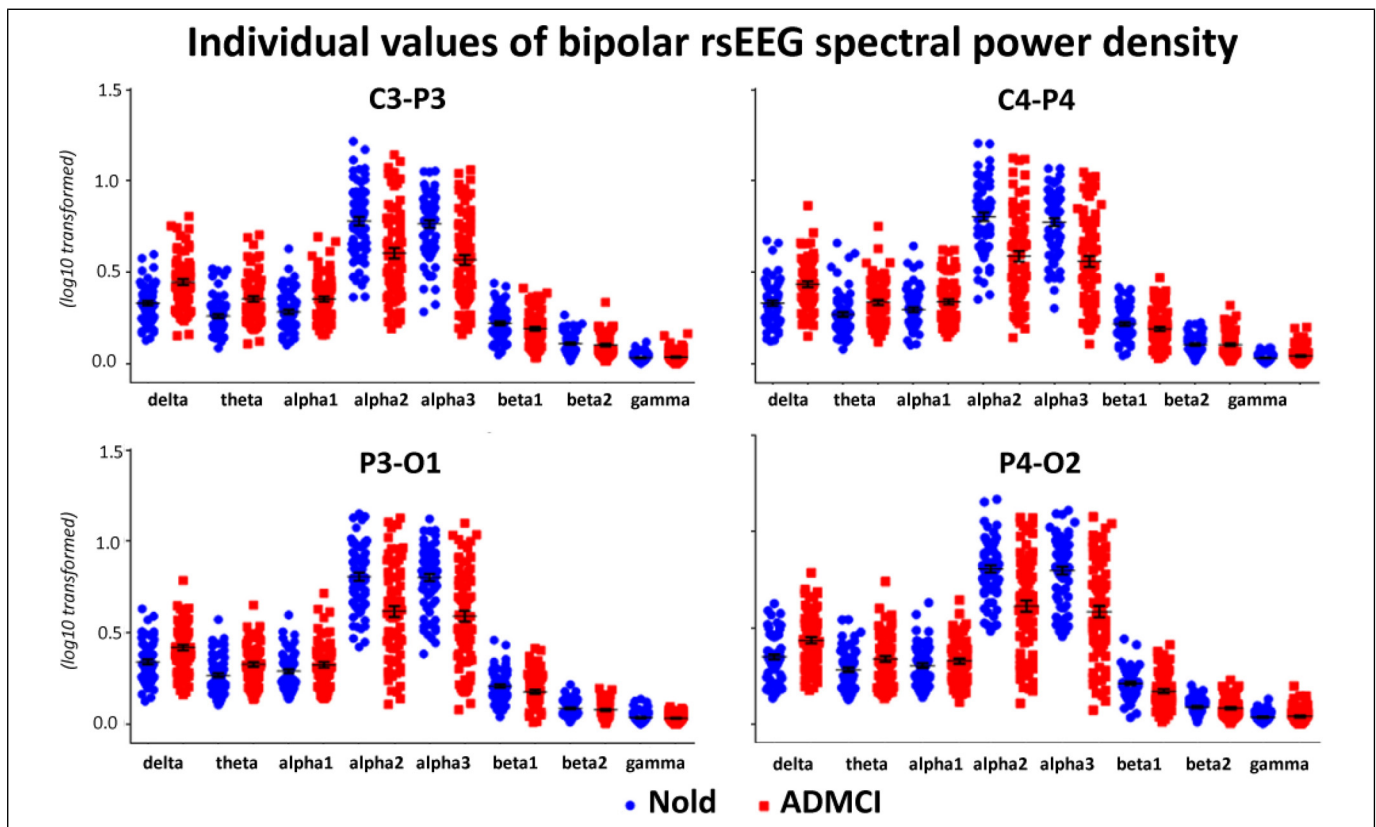
**Figure 2.** Individual values (log-10 transformed) of the bipolar rsEEG spectral power density estimated at the four centro-parietal and parieto-occipital bipolar channels (C3-P3, C4-P4, P3-O1, and P4-O2; mean across subjects, log-10 transformed) at the different frequency band (ie De = delta, Th = theta, A1 = alpha1, A2 = alpha2, A3 = alpha3, B1 = beta1, B2 = beta2, Ga = gamma). Noteworthy, the Grubbs' test showed no outliers from those individual values of the bipolar rsEEG spectral power density (arbitrary threshold of p < 0.001).

alpha 3 frequencies, ie, the A2/Th and A3/Th (from 0.75 to 0.81). The ROC curves of those best results are plotted in Figure 5. Table 3 illustrates all relevant results (AUROC > 0.7).

## Discussion

Can one capture abnormalities of rsEEG spectral biomarkers in ADMCI patients at the group and individual levels using just a few scalp bipolar leads in the framework of health remote monitoring? To answer this question, we performed a standard spectral FFT analysis of rsEEG data at the delta, theta, and alpha frequency bands using 6 monopolar scalp electrodes to derive bipolar C3-P3, C4-P4, P3-O1, and P4-O2 spectral markers. Classification accuracy of rsEEG biomarkers was measured by the area under the receiver operating characteristic (AUROC) curve.

Results showed that compared to the Nold group, the ADMCI group showed increased delta power density and decreased alpha power density at the C3-P3, C4-P4, P3-O1, and P4-O2 bipolar channels. Increased theta power density for ADMCI patients was observed only at the C3-P3 bipolar channel. Best classification accuracy between the ADMCI and Nold individuals reached 81%

(area under the receiver operating characteristic curve) using Alpha2/Theta power density computed at the C3-P3 bipolar channel.

These results suggest that a simple bipolar configuration acquiring rsEEG rhythms from a few scalp electrodes showed differences between Nold seniors and ADMCI patients at the group and individual levels. These results align with previous evidence by our research workgroup grounded on rsEEG recordings using a standard clinical electrode montage with 19 scalp electrodes (ie, 10-20 montage system). In those previous studies, when compared to Nold control seniors, abnormalities in rsEEG rhythms were observed in groups of AD patients, at delta, theta, and alpha frequency bands. Specifically, groups of ADD and ADMCI patients were characterized over the Nold control seniors by the decrease in alpha power density or estimated cortical source activities and decreased theta-delta power density or estimated cortical source activities.[6–12] At the individual level, previous rsEEG studies reported that the ratio of rsEEG power density at delta, theta, and alpha frequency bands was able to classify ADMCI patients at the individual level with an accuracy of around 80% (AUROC).
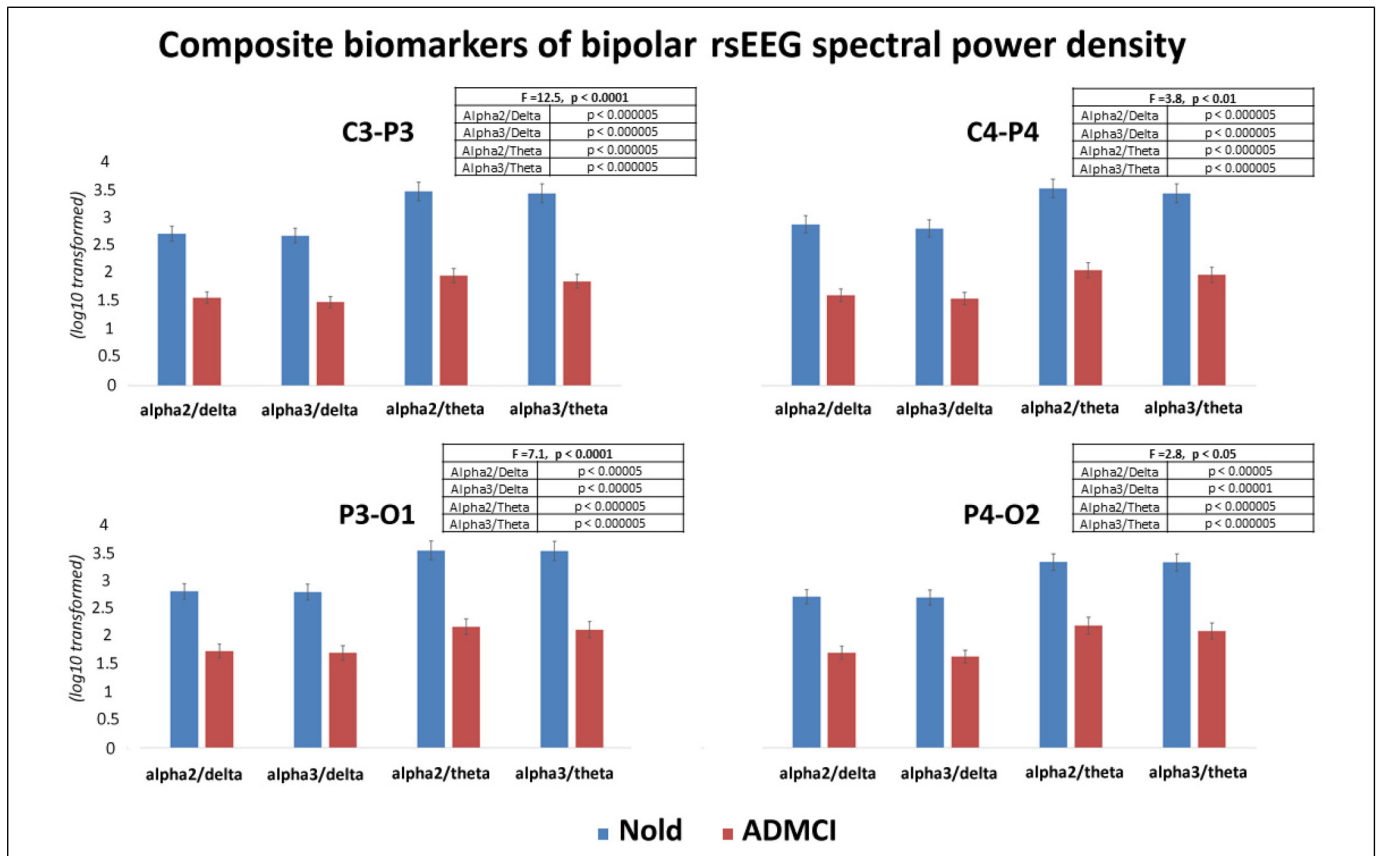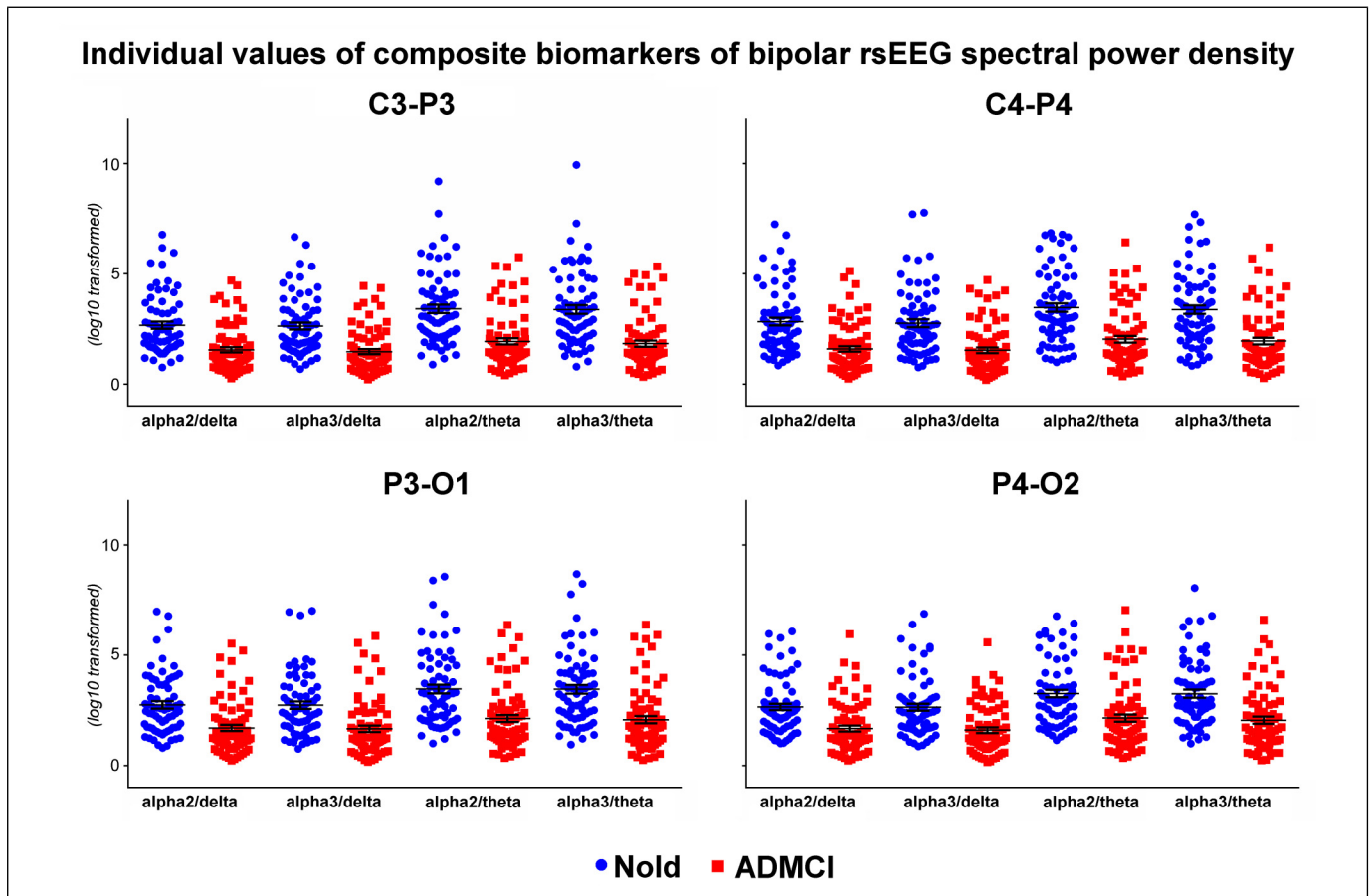
**Figure 3.** Bipolar rsEEG spectral power density estimated at the four centro-parietal and parieto-occipital bipolar channels (C3-P3, C4-P4, P3-O1, and P4-O2; mean across subjects, log-10 transformed) relative to statistically significant ANOVA interactions (p < 0.0001; Fisher test values reported in each sub-figure) among the factors Group (Nold and ADMCI) and Biomarkers (A2/De, A3/De, A2/Th, and A3/Th). Legend: the tables in each sub-figure indicate the frequency bands in which the Bipolar rsEEG spectral power density differed between Nold and ADMCI groups (p < 0.05 corrected = p < 0.0125).

Other research consortia obtained similar results with rsEEG recordings in standard hospital settings.[41–46] A recent large-scale clinical study in people diagnosed with subjective cognitive decline (SCD), MCI, and AD, found a significant correlation between increased delta and theta global field power (GFP; a single measure of the generalized EEG amplitude) and reduced global field synchronization (GFS; the global amount of instantaneous phase-locked synchronization of oscillating neuronal networks across the scalp) with lower CSF Aβ42 and higher p-tau and t-tau levels.[47] These findings implicate the usefulness of rsEEG features as early noninvasive biomarkers of AD.

The use of rsEEG spectral biomarkers derived from a few scalp electrodes for monitoring ADMCI patients may use rsEEG raw data collected by low-cost portable EEG systems installed in small local Public Health services near underserved populations in lower- and middle-income countries. Several studies have explored the potential use of mobile EEG devices in neurological diseases.[48–51] Furthermore, low-cost configurations with 4–6 EEG recording channels are already available for a few thousand Euros.

Notably, the present results relied on a few standard scalp rsEEG recordings in hospital settings, so they may not be generalized to rsEEG activity collected with low-quality EEG systems. Therefore, all low-cost EEG systems with few scalp electrodes should receive a specific validation about the quality of rsEEG activity recorded during an experimental session lasting about 5 min for the eyes closed condition and 5 min for the eyes open condition.

Low-cost rsEEG recordings from a few electrodes may aid in deriving clinically reliable estimates of brain dysfunctions in the regulation of quiet vigilance, reflecting the effect of AD progression from early prodromal stages with very mild cognitive deficits to dementia. In this line, rsEEG recordings at the point of care (eg, local centers for the surveillance of dementing disorders in aging, family medical audits, residency homes) may allow extensive population screening to timely reveal an incipient decline in cortical brain functioning in quiet vigilance. Of course, only standard diagnostic in-vivo biomarkers of AD neuropathology (eg, CSF, amyPET. etc) may assess the final diagnosis of AD, but with a clear cost breakdown related to unnecessary medical examinations.

**Figure 4.** Individual values (log-10 transformed) of the bipolar rsEEG spectral power density estimated at the four centro-parietal and parieto-occipital bipolar channels (C3-P3, C4-P4, P3-O1, and P4-O2; mean across subjects, log-10 transformed) for the different composite biomarkers (ie A2/De = alpha2/delta, A3/De = alpha3/delta, A2/Th = alpha2/theta, and A3/Th = alpha3/theta). Noteworthy, the Grubbs' test showed no outliers from those individual values of the bipolar rsEEG spectral power density (arbitrary threshold of p < 0.001).

## Methodological Remarks

Even though there is increasing evidence and interest in applying rsEEG low-channel devices for clinical telehealth purposes, future development, and actual application in ADMCI patients. should consider different limitations.

Mobile systems encompass hardware solutions transforming EEG systems into one of the most accessible neuroscientific tools.[52] These systems may consist of small, lightweight amplifiers alongside wireless transmission, contributing to increased portability. They can also reduce power and remote transmission resources by using more channels and then compressing them at the acquisition phase.[53] In these systems, algorithms may allow data logging and transmission from several channels for specific periods.[15] For example, an exciting study described an ear-EEG portable system, able to record EEG from the ear channel.[54] Beyond the unquestionable wearability and discreteness, some critical elements may be the limited power autonomy, poor spatial resolution,

and real-world noisy EEG signals for the application to ADMCI patients.[54]

Recent developments in dry electrodes[55] could further decrease preparation time, removing the requirement to apply a conductive gel/saline patch and prepare the skin as required in traditional EEG to reduce skin-electrode contact impedance. However, as the signal quality depends on the correct electrode positioning, meticulous attention should be paid to obtain reliable measures. It is necessary to train the patient/caregiver in setting up the EEG mobile system and performing preliminary tests to assess the validity of the recorded EEG signals.

Nowadays, every commercially available laptop may install software for EEG data acquisition and preprocessing. The whole acquisition chain, including the rsEEG electrodes, the amplifier, and the cables for the interconnection between them and the computer, would be exceptionally light and easy to use in case of a low number of channels are recorded.

With a well-diffuse and stable internet connection, the data storage may be on cloud servers, allowing researchers to

## ROC curves of ADMCI vs Nold individuals classification
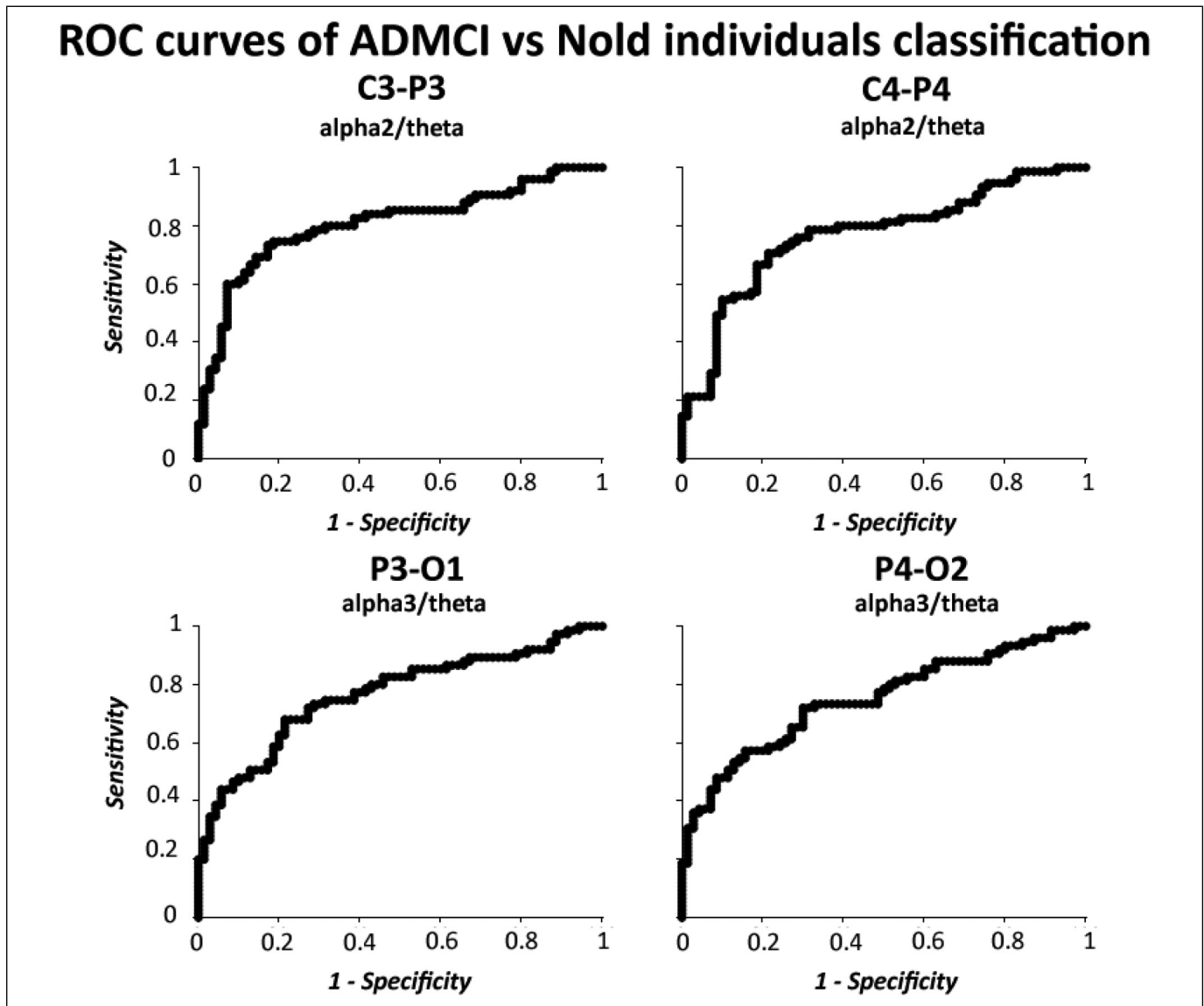


**Figure 5.** Receiver operating characteristic (ROC) curves illustrating the best result for the classification of the ADMCI versus Nold individuals based on the following composite biomarkers of bipolar rsEEG spectral power density: alpha2/theta at C3-P3 (area under the ROC – AUROC - curve = 0.81) and C4-P4 (AUROC = 0.78) channel, and alpha3/theta at P3-O1 (AUROC = 0.77) and P4-O2 (AUROC = 0.75) channels. An AUROC curve > 0.7 which corresponds to a moderate to a good performance of the classification. The sensitivity shows the "true positive rate" and specificity the "true negative rate" (1-specificity shows the "false positive rate"), in the signal detection theory.

remotely access and download the raw EEG data for subsequent analysis. In the future, using a tablet or smartphone will further simplify these processes.

Considering the above points, applying these portable rsEEG devices has revealed limitations regarding the validity and reproducibility of the acquired measures. The installation at a patient's home implicates further restrictions on the patient's ability in self-application and management, as well as security issues regarding data transmission and storage.

Further studies are required to determine better usability (it may be challenging even for healthy elderly), validity, and reproducibility of the rsEEG measures derived from portable low-channel

density EEG systems for use at ADMCI patients' homes. Using those systems in patients' homes may be especially useful in ADMCI patients (compared to AD patients with dementia) as they should remain autonomous for years in their homes. Their good cognitive status may enable them to use those systems in their homes to produce valid and reliable rsEEG biomarkers for monitoring brain functions over time. Of course, before these applications, future studies will have to evaluate rsEEG biomarkers not only about the present "gold standard" but also:

1. Calculating the accuracy in the classification between Nold and ADMCI patients.

**Table 3.** The Best Results (AUROC Curve Value Higher than 0.7 Which Corresponds to a Moderate to a Good Performance of the Classification) for ADMCI Versus Nold Classification. The sensitivity (ie, "True Positive rate" in the Signal Detection Theory), Specificity (ie, "True Negative Rate" in the Signal Detection Theory), Accuracy (ie, the Weighted Average of the Sensitivity and Specificity Values), and Area Under the ROC (AUROC) Curve Measured the Performance of the Binary Classification. Best Classification Results are Highlighted in Bold Type.

**Bipolar C3-P3**

| | Sensitivity% | Specificity% | Accuracy% | AUROC |
|---|---|---|---|---|
| **Delta** | 70.7 | 74.3 | 72.4 | 0.75 |
| **Theta** | 52.0 | 87.1 | 69.0 | 0.73 |
| **Alpha2** | 56.0 | 81.4 | 68.3 | 0.71 |
| **Alpha3** | 58.7 | 85.7 | 71.7 | 0.75 |
| **Alpha2/ Delta** | 60.0 | 92.9 | 75.9 | 0.79 |
| **Alpha3/ Delta** | 68.0 | 85.7 | 76.5 | 0.79 |
| **Alpha2/ Theta** | **73.3** | **82.9** | **77.9** | **0.81** |
| **Alpha3/ Theta** | 64.0 | 88.6 | 75.9 | 0.81 |

**Bipolar P3-O1**

| | Sensitivity% | Specificity% | Accuracy% | AUROC |
|---|---|---|---|---|
| **Delta** | | | | < 0.7 |
| **Theta** | | | | < 0.7 |
| **Alpha2** | 62.7 | 73.9 | 68.1 | 0.72 |
| **Alpha3** | 65.3 | 76.8 | 70.9 | 0.74 |
| **Alpha2/ Delta** | 56.0 | 85.7 | 70.3 | 0.75 |
| **Alpha3/ Delta** | 70.7 | 75.7 | 73.1 | 0.75 |
| **Alpha2/ Theta** | 52.0 | 94.3 | 72.4 | 0.76 |
| **Alpha3/ Theta** | **68.0** | **78.6** | **73.1** | **0.77** |

**Bipolar C4-P4**

| | Sensitivity% | Specificity% | Accuracy% | AUROC |
|---|---|---|---|---|
| **Delta** | 65.3 | 74.3 | 69.7 | 0.72 |
| **Theta** | | | | < 0.7 |
| **Alpha2** | 68.0 | 72.9 | 70.3 | 0.75 |
| **Alpha3** | 56.0 | 84.3 | 69.7 | 0.74 |
| **Alpha2/ Delta** | 58.7 | 90.0 | 73.8 | 0.78 |
| **Alpha3/Delta** | 66.7 | 78.6 | 72.4 | 0.78 |
| **Alpha2/ Theta** | **70.7** | **78.6** | **74.5** | **0.78** |
| **Alpha3/ Theta** | 69.3 | 82.9 | 75.9 | 0.77 |

**Bipolar P4-O2**

| | Sensitivity% | Specificity% | Accuracy% | AUROC |
|---|---|---|---|---|
| **Delta** | | | | < 0.7 |
| **Theta** | | | | < 0.7 |
| **Alpha2** | 61.3 | 84.3 | 72.4 | 0.73 |
| **Alpha3** | 74.7 | 68.6 | 71.7 | 0.75 |
| **Alpha2/ Delta** | 58.7 | 87.1 | 72.4 | 0.75 |
| **Alpha3/ Delta** | 60.0 | 87.1 | 73.1 | 0.75 |
| **Alpha2/ Theta** | 78.7 | 67.1 | 73.1 | 0.75 |
| **Alpha3/ Theta** | **72.0** | **70.0** | **71.0** | **0.75** |

2. Correlating those measures with biofluid and neuroimaging biomarkers of AD.
3. Assessing their sensitivity to the AD progression in longitudinal cohort studies from MCI stage to dementia.

## Conclusions

In the present study, we evaluated whether abnormalities of rsEEG rhythms can be observed even from a smaller number of scalp electrodes in ADMCI patients towards the use of low-cost devices in low- and middle-income countries in the framework of health monitoring applications. Specifically, we tested rsEEG biomarkers based on a few scalp electrodes and a standard hospital setting for the discrimination of Nold and ADMCI seniors to be used as a "gold standard" for a new generation of rsEEG biomarkers derived from low-cost portable EEG systems, characterized by a minimal number of channels and low consumption of energy. If confirmed, these results will justify their potential candidature as a "gold standard" for a new generation of rsEEG biomarkers derived from low-cost portable EEG systems characterized by few channels and low energy consumption.

To this aim, we included the clinical and rsEEG data from an international archive acquired in hospital settings (10-20 electrode montage) from 75 ADMCI participants and 70 age-, education-, and sex-matched Nold seniors. Standard spectral FFT analysis of rsEEG data for individual delta, theta, and alpha frequency bands was computed from 6 monopolar scalp electrodes to derive bipolar C3-P3, C4-P4, P3-O1, and P4-O2 spectral markers. The ADMCI group showed increased delta power density and decreased alpha power density at the C3-P3, C4-P4, P3-O1, and P4-O2 bipolar channels. Increased theta power density for ADMCI patients was observed only at the C3-P3 bipolar channel. Best classification accuracy between the ADMCI and Nold individuals reached 81% (area under the receiver operating characteristic curve) using Alpha2/Theta power density computed at the C3-P3 bipolar channel.

Standard rsEEG power density computed from six posterior bipolar channels characterized ADMCI status, thus encouraging its applicability in future clinical health monitoring in those patients along the disease progression until dementia using low-cost EEG systems in lower- and middle-income countries.

## Ethical Approval

## ORCID iDs

Claudio Del Percio ⓘD https://orcid.org/0000-0001-8805-2945
Susanna Lopez ⓘD https://orcid.org/0000-0002-3568-2668
Bahar Güntekin ⓘD https://orcid.org/0000-0002-0860-0524
Görsev Yener ⓘD https://orcid.org/0000-0002-7756-4387

## References

1. Jack CRJr, Bennett DA, Blennow K, et al. NIA-AA Research framework: toward a biological definition of Alzheimer's disease. *Alzheimers Dement*. 2018;14(4):535-562. doi:10.1016/j.jalz.2018.02.018.
2. Babiloni C, Arakaki X, Azami H, et al. Measures of resting state EEG rhythms for clinical trials in Alzheimer's disease: recommendations of an expert panel. *Alzheimers Dement*. 2021;17(9):1528-1553. doi:10.1002/alz.12311.
3. Klass DW, Brenner RP. Electroencephalography of the elderly. *J Clin Neurophysiol*. 1995;12(2):116-131. doi:10.1097/00004691-199503000-00002.
4. Rossini PM, Miraglia F, Alù F, et al. Neurophysiological hallmarks of neurodegenerative cognitive decline: the study of brain connectivity as A biomarker of early dementia. *J Pers Med*. 2020;10(2):34. Published 2020 Apr 30. doi:10.3390/jpm10020034.
5. Hubbard O, Sunde D, Goldensohn ES. The EEG in centenarians. *Electroencephalogr Clin Neurophysiol*. 1976;40(4):407-417. doi:10.1016/0013-4694(76)90192-9.
6. Babiloni C, Binetti G, Cassetta E, et al. Sources of cortical rhythms change as a function of cognitive impairment in pathological aging: a multicenter study. *Clin Neurophysiol*. 2006;117(2):252-268. doi:10.1016/j.clinph.2005.09.019.
7. Galluzzi S, Marizzoni M, Babiloni C, et al. Clinical and biomarker profiling of prodromal Alzheimer's disease in work package 5

of the innovative medicines initiative PharmaCog project: a 'European ADNI study'. *J Intern Med*. 2016;279(6):576-591. doi:10.1111/joim.12482.

8. Jovicich J, Babiloni C, Ferrari C, et al. Two-Year longitudinal monitoring of amnestic mild cognitive impairment patients with prodromal Alzheimer's disease using topographical biomarkers derived from functional magnetic resonance imaging and electroencephalographic activity. *J Alzheimers Dis*. 2019;69(1):15-35. doi:10.3233/JAD-180158.

9. Marizzoni M, Ferrari C, Macis A, et al. Biomarker matrix to track short term disease progression in amnestic mild cognitive impairment patients with prodromal Alzheimer's disease. *J Alzheimers Dis*. 2019;69(1):49-58. doi:10.3233/JAD-181016.

10. Babiloni C, Ferri R, Noce G, et al. Abnormalities of cortical sources of resting state alpha electroencephalographic rhythms are related to education attainment in cognitively unimpaired seniors and patients with Alzheimer's disease and amnesic mild cognitive impairment. *Cereb Cortex*. 2021;31(4):2220-2237. doi:10.1093/cercor/bhaa356.

11. Babiloni C, Ferri R, Noce G, et al. Resting state alpha electroencephalographic rhythms are differently related to aging in cognitively unimpaired seniors and patients with Alzheimer's disease and amnesic mild cognitive impairment. *J Alzheimers Dis*. 2021;82(3):1085-1114. doi:10.3233/JAD-201271.

12. Babiloni C, Noce G, Ferri R, et al. Resting state alpha electroencephalographic rhythms are affected by sex in cognitively unimpaired seniors and patients with Alzheimer's disease and amnesic mild cognitive impairment: a retrospective and exploratory study. *Cereb Cortex* 2022;32(10):2197-2215. doi: 10.1093/cercor/bhab348.

13. Rogers JM, Johnstone SJ, Aminov A, Donnelly J, Wilson PH. Test-retest reliability of a single-channel, wireless EEG system. *Int J Psychophysiol*. 2016;106:87-96. doi:10.1016/j.ijpsycho.2016.06.006.

14. Troller-Renfree SV, Morales S, Leach SC, et al. Feasibility of assessing brain activity using mobile, in-home collection of electroencephalography: methods and analysis. *Dev Psychobiol*. 2021;63(6):e22128. doi:10.1002/dev.22128.

15. Casson A, Yates D, Smith S, Duncan J, Rodriguez-Villegas E. Wearable electroencephalography. What is it, why is it needed, and what does it entail? *IEEE Eng Med Biol Mag*. 2010;29(3):44-56. doi:10.1109/MEMB.2010.936545.

16. McWilliams EC, Barbey FM, Dyer JF, et al. Feasibility of repeated assessment of cognitive function in older adults using a wireless, Mobile, dry-EEG headset and tablet-based games. *Front Psychiatry*. 2021;12:574482.

17. Albert MS, DeKosky ST, Dickson D, et al. The diagnosis of mild cognitive impairment due to Alzheimer's disease: recommendations from the national institute on aging-Alzheimer's association workgroups on diagnostic guidelines for Alzheimer's disease. *Alzheimers Dement*. 2011;7(3):270-279. doi:10.1016/j.jalz.2011.03.008.

18. Morris JC. The clinical dementia rating (CDR): current version and scoring rules. *Neurology*. 1993;43(11):2412-2414. doi:10.1212/wnl.43.11.2412-a.

19. Wechsler D. WMS-R: Wechsler Memory Scale-Revised: Manual. 1984. San Antonio, TX: Psychological Corporation.

20. Brown LM, Schinka JA. Development and initial validation of a 15-item informant version of the geriatric depression scale. *Int J Geriatr Psychiatry*. 2005;20(10):911-918. doi:10.1002/gps.1375.

21. Rosen WG, Terry RD, Fuld PA, Katzman R, Peck A. Pathological verification of ischemic score in differentiation of dementias. *Ann Neurol*. 1980;7(5):486-488. doi:10.1002/ana.410070516.

22. Osterrieth PA. Le test de copie d'une figure complexe: contribution a l'étude de la perception et de la memoire [copying a complex figure: contributions to the study of perception and memory]. *Arch Psychol (Geneve)*. 1944;30(30):203-353.

23. Mattsson N, Andreasson U, Persson S, et al. The Alzheimer's association external quality control program for cerebrospinal fluid biomarkers. *Alzheimers Dement*. 2011;7(4):386-395.e6. doi: 10.1016/j.jalz.2011.05.2243.

24. Folstein MF, Folstein SE, McHugh PR. "Mini-mental state". A practical method for grading the cognitive state of patients for the clinician. *J Psychiatr Res*. 1975;12(3):189-198. doi:10.1016/0022-3956(75)90026-6.

25. Rosen WG, Mohs RC, Davis KL. A new rating scale for Alzheimer's disease. *Am J Psychiatry*. 1984;141(11):1356-1364. doi:10.1176/ajp.141.11.1356.

26. Estévez-González A, Kulisevsky J, Boltes A, Otermín P, García-Sánchez C. Rey verbal learning test is a useful tool for differential diagnosis in the preclinical phase of Alzheimer's disease: comparison with mild cognitive impairment and normal aging. *Int J Geriatr Psychiatry*. 2003;18(11):1021-1028. doi: 10.1002/gps.1010. PMID: 14618554.

27. Reitan RM. Validity of the trail making test as an indicator of organic brain damage. *Percept Mot Skills*. 1958;8(3):271-276.

28. Novelli G, Papagno C, Capitani E, Laiacona M, Vallar G, Cappa SF. Tre test clinici di ricerca e produzione lessicale. Taratura su soggetti normali. *Arch Psicol Neurol Psichiatr*. 1986;47(4): 477-506.

29. Freedman M, Leach L, Kaplan E, Winoucur G, Shulman KJ, Delis DC. *Clock Drawing. A neuropsichological analysis*. Oxford University Press; 1994.

30. Sirály E, Szabó Á, Szita B, et al. Monitoring the early signs of cognitive decline in elderly by computer games: an MRI study. *PLoS One*. 2015;10(2):e0117918.

31. Babiloni C, Del Percio C, Lizio R, et al. Abnormalities of cortical neural synchronization mechanisms in subjects with mild cognitive impairment due to Alzheimer's and Parkinson's diseases: an EEG study. *J Alzheimers Dis*. 2017;59(1):339-358. doi:10.3233/JAD-160883.

32. Babiloni C, Del Percio C, Lizio R, et al. Abnormalities of resting state cortical EEG rhythms in subjects with mild cognitive impairment due to Alzheimer's and Lewy body diseases. *J Alzheimers Dis*. 2018;62(1):247-268. doi:10.3233/JAD-170703.

33. Babiloni C, Del Percio C, Pascarelli MT, et al. Abnormalities of functional cortical source connectivity of resting-state electroencephalographic alpha rhythms are similar in patients with mild cognitive impairment due to Alzheimer's and Lewy body diseases. *Neurobiol Aging*. 2019;77:112-127. doi:10.1016/j.neurobiolaging.2019.01.013.

34. Pascual-Marqui RD. Discrete, 3D distributed, linear imaging methods of electric neuronal activity. Part 1: exact, zero error localization. arXiv:0710.3341, 2007-October-17, http://arxiv.org/pdf/0710.3341.

35. Klimesch W. EEG Alpha and theta oscillations reflect cognitive and memory performance: a review and analysis. *Brain Res Brain Res Rev*. 1999;29(2-3):169-195. doi:10.1016/s0165-0173(98)00056-3.

36. Klimesch W. α-band oscillations, attention, and controlled access to stored information. *Trends Cogn Sci*. 2012;16(12):606-617. doi:10.1016/j.tics.2012.10.007.

37. Klimesch W, Doppelmayr M, Russegger H, Pachinger T, Schwaiger J. Induced alpha band power changes in the human EEG and attention. *Neurosci Lett*. 1998;244(2):73-76. doi:10.1016/s0304-3940(98)00122-0.

38. Klimesch W, Doppelmayr M, Russegger H, Pachinger T. Theta band power in the human scalp EEG and the encoding of new

information. *Neuroreport*. 1996;7(7):1235-1240. doi:10.1097/00001756-199605170-00002.

39. Pfurtscheller G, Lopes da Silva FH. Event-related EEG/MEG synchronization and desynchronization: basic principles. *Clin Neurophysiol*. 1999;110(11):1842-1857. doi:10.1016/s1388-2457(99)00141-8.

40. DeLong ER, DeLong DM, Clarke-Pearson DL. Comparing the areas under two or more correlated receiver operating characteristic curves: a nonparametric approach. *Biometrics*. 1988;44(3):837-845.

41. Prinz PN, Vitiello MV. Dominant occipital (alpha) rhythm frequency in early stage Alzheimer's disease and depression. *Electroencephalogr Clin Neurophysiol*. 1989;73(5):427-432. doi:10.1016/0013-4694(89)90092-8.

42. Huang C, Wahlund L, Dierks T, Julin P, Winblad B, Jelic V. Discrimination of Alzheimer's disease and mild cognitive impairment by equivalent EEG sources: a cross-sectional and longitudinal study. *Clin Neurophysiol*. 2000;111(11):1961-1967. doi:10.1016/s1388-2457(00)00454-5.

43. Hughes SW, Crunelli V. Thalamic mechanisms of EEG alpha rhythms and their pathological implications. *Neuroscientist*. 2005;11(4):357-372.

44. de Haan W, Stam CJ, Jones BF, Zuiderwijk IM, van Dijk BW, Scheltens P. Resting-state oscillatory brain dynamics in Alzheimer disease. *J Clin Neurophysiol*. 2008;25(4):187-193. doi:10.1097/WNP.0b013e31817da184.

45. Poil SS, de Haan W, van der Flier WM, Mansvelder HD, Scheltens P, Linkenkaer-Hansen K. Integrative EEG biomarkers predict progression to Alzheimer's disease at the MCI stage. *Front Aging Neurosci*. 2013;5:58. Published 2013 Oct 3. doi:10.3389/fnagi.2013.00058.

46. Özbek Y, Fide E, Yener GG. Resting-state EEG alpha/theta power ratio discriminates early-onset Alzheimer's disease from healthy controls. *Clin Neurophysiol*. 2021;132(9):2019-2031. doi:10.1016/j.clinph.2021.05.012.

47. Smailovic U, Koenig T, Kåreholt I, et al. Quantitative EEG power and synchronization correlate with Alzheimer's disease CSF biomarkers. *Neurobiol Aging*. 2018;63:88-95. doi:10.1016/j.neurobiolaging.2017.11.005.

48. Casson AJ. Wearable EEG and beyond. *Biomed Eng Lett*. 2019;9(1):53-71. Published 2019 Jan 4. doi:10.1007/s13534-018-00093-6.

49. Park S, Han CH, Im CH. Design of wearable EEG devices specialized for passive brain-computer interface applications. *Sensors (Basel)*. 2020;20(16):4572. Published 2020 Aug 14. doi:10.3390/s20164572.

50. Carvalho D, Mendes T, Dias AI, Leal A. Interictal spike quantification in continuous spike-wave of sleep (CSWS): clinical usefulness of a wearable EEG device. *Epilepsy Behav*. 2020;104(Pt A):106902. doi:10.1016/j.yebeh.2020.106902.

51. Byrom B, McCarthy M, Schueler P, Muehlhausen W. Brain monitoring devices in neuroscience clinical research: the potential of remote monitoring using sensors, wearables, and Mobile devices. *Clin Pharmacol Ther*. 2018;104(1):59-71. doi:10.1002/cpt.1077.

52. Lau-Zhu A, Lau MPH, McLoughlin G. Mobile EEG in research on neurodevelopmental disorders: opportunities and challenges. *Dev Cogn Neurosci*. 2019;36:100635. doi:10.1016/j.dcn.2019.100635.

53. Morabito FC, Labate D, Bramanti A, et al. Enhanced compressibility of EEG signal in Alzheimer's disease patients. *IEEE Sensors J*. 2013;13(9):3255-3262. doi: 10.1109/JSEN.2013.2263794.

54. Looney D, Kidmose P, Park C, et al. The in-the-ear recording concept: user-centered and wearable brain monitoring. *IEEE Pulse*. 2012;3(6):32-42.

55. Liao LD, Chen CY, Wang IJ, et al. Gaming control using a wearable and wireless EEG-based brain-computer interface device with novel dry foam-based sensors. *J Neuroeng Rehabil*. 2012;9:5. doi: 10.1186/1743-0003-9-5.